

# The Near-Infrared and Optical Spectra of Methane Dwarfs and Brown Dwarfs

Adam Burrows<sup>1</sup>, M.S. Marley<sup>2</sup>, & C.M. Sharp<sup>1</sup>

## ABSTRACT

We identify the pressure-broadened red wings of the saturated potassium resonance lines at 7700 Å as the source of anomalous absorption seen in the near-infrared spectra of Gliese 229B and, by extension, of methane dwarfs in general. The WFPC2 *I* band measurement of Gliese 229B is also consistent with this hypothesis. Furthermore, a combination of the blue wings of this K I resonance doublet, the red wings of the Na D lines at 5890 Å, and, perhaps, the Li I line at 6708 Å can explain in a natural way the observed WFPC2 *R* band flux of Gliese 229B. Hence, we conclude that the neutral alkali metals play a central role in the near-infrared and optical spectra of methane dwarfs and that their lines have the potential to provide crucial diagnostics of brown dwarf properties.

The slope of the spectrum from 0.8  $\mu\text{m}$  to 0.9  $\mu\text{m}$  for the Sloan methane dwarf, SDSS 1624+00, is shallower than that for Gliese 229B and its Cs lines are weaker. From this, we conclude that its atmosphere is tied to a lower core entropy or that its K and Cs abundances are smaller, with a preference for the former hypothesis. We speculate on the systematics of the near-infrared and optical spectra of methane dwarfs, for a given mass and composition, that stems from the progressive burial with decreasing  $T_{\text{eff}}$  of the alkali metal atoms to larger pressures and depths.

Moreover, we surmise that those extrasolar giant planets (EGPs) that achieve  $T_{\text{eff}}$  in the 800–1300 K range due to stellar insolation will show signatures of the neutral alkali metals in their albedo and reflection spectra. We estimate that, due predominantly to absorption by Na D lines, the geometric albedo of the EGP  $\tau$  Boo b at  $\lambda = 0.48 \mu\text{m}$  is  $< 0.1$ , consistent with the new (and low) upper limit of 0.3 recently obtained by Charbonneau *et al.* (1999).

*Subject headings:* brown dwarfs, Gliese 229B, SDSS 1624+00, methane dwarfs, T dwarfs, extrasolar giant planets, alkali metals, atmospheres, non-gray spectral synthesis

## 1. Introduction

The discovery of Gliese 229B in 1995 was a milestone in the study of brown dwarfs, providing the first bona fide object with an effective temperature ( $T_{\text{eff}} \sim 950 \text{ K}$ ) that was unambiguously

---

<sup>1</sup>Department of Astronomy and Steward Observatory, The University of Arizona, Tucson, AZ 85721

<sup>2</sup>Department of Astronomy, New Mexico State University, Box 30001/Dept. 4500, Las Cruces NM 88003

substellar (Nakajima *et al.* 1995; Oppenheimer *et al.* 1995). It also validated in dramatic fashion the allied theoretical and observational efforts of the many groups around the world that were engaged in brown dwarf research and started a race to discover and understand brown dwarfs that shows no sign of abating. Indeed, *seven* similar substellar mass objects, the so-called “T” or “methane” dwarfs, have since been discovered in the field by the Sloan Digital Sky Survey (Strauss *et al.* 1999; Tsvetanov *et al.* 1999), by the 2MASS survey (Burgasser *et al.* 1999), and by the NTT/VLT (Cuby *et al.* 1999). Superficially, these all seem to be clones of Gl 229B, but there are subtle spectral differences that no doubt reflect true differences in mass, metallicity, and effective temperature. In addition to this flurry of brown dwarf discoveries, the first new stellar spectral class in almost 100 years, the “L type,” has been defined, with  $\sim$ 100 members having been found to date by 2MASS (Kirkpatrick *et al.* 1999) and DENIS (Delfosse *et al.* 1997; Tinney *et al.* 1998). These objects are characterized by the clear onset of refractory heavy metal depletion, in particular that of titanium and vanadium, and by the growth in strength of the alkali metal lines of cesium, potassium, rubidium, and sodium in their optical and near-infrared spectra. L dwarfs also show distinct bands of FeH and CrH. Such transitions in chemical makeup with decreasing  $T_{\text{eff}}$  are in keeping with theoretical predictions of the molecular constituents of substellar atmospheres (Burrows and Sharp 1999; Fegley and Lodders 1996) that can serve to anchor and define the sequence of L dwarf spectral subtypes (Kirkpatrick *et al.* 1999). The L dwarfs have  $T_{\text{eff}}$ s from  $\sim$ 1500 K to  $\sim$ 2000 K and constitute the spectroscopic link between M dwarfs and Gl 229B-like objects (Kirkpatrick *et al.* 1999). Many L dwarfs are also brown dwarfs (with masses below the stellar boundary at  $\sim$ 0.075  $M_{\odot}$ ), but some will turn out to be stars very near the stellar edge. The current ambiguity reflects the newness of this subject.

In this paper, we address T (methane) dwarf spectra in the optical and near infrared, focussing predominantly on Gl 229B as the prototype. Marley *et al.* (1996) and Allard *et al.* (1996) analyzed the full spectrum of Gl 229B (Oppenheimer *et al.* 1995; Geballe *et al.* 1996; Oppenheimer *et al.* 1998; Schultz *et al.* 1998) and obtained reasonable fits from the *J* band ( $\sim$  1.2  $\mu\text{m}$ ) through the *N* band ( $\sim$  10  $\mu\text{m}$ ). They concluded that its  $T_{\text{eff}}$  was  $\sim$ 900–1000 K and that its gravity ( $g$ ) was  $\sim 3 \times 10^4 - 10^5 \text{ cm s}^{-2}$ . The gravity error bars were large and translated into a factor of  $\sim$ 2–3 uncertainty in its inferred mass and age. They also concluded that the atmosphere of Gl 229B is indeed depleted in the refractory heavy elements, such as Al, Si, Ca, Fe, and Mg, just as the theory of condensate formation and rainout in cool molecular atmospheres would suggest, and that its spectrum longward of  $\sim$ 1  $\mu\text{m}$  can be fit, in the main, by a simple mixture of  $\text{H}_2\text{O}$ ,  $\text{CH}_4$ , and  $\text{H}_2$ . (Noll, Geballe, and Marley (1997) have detected CO at 4.67  $\mu\text{m}$  in Gl 229B as well.) However, neither Marley *et al.* (1996) nor Allard *et al.* (1996) were able to fit the near-infrared observations between 0.8  $\mu\text{m}$  and 1.0  $\mu\text{m}$  and the theoretical excesses in flux ranged from 10 to 100. The line marked “Clear” in Figure 1 demonstrates the typical discrepancy between theory, that otherwise fits rather well at longer wavelengths, and the observed spectrum of Gl 229B (Leggett *et al.* 1999). Clearly, some ingredient is absorbing in the blue, creating a very steep spectrum with a deep red (infrared) cast.

Attempts to fit this problematic spectral interval were made by Golimowski *et al.* (1998), who invoked a Tsuji *et al.* (1996) spectrum that retained TiO in the atmosphere to take full advantage of TiO’s strong absorption in the blue, and Griffith *et al.* (1998), who hypothesized that a population of small photochemical haze particles analogous to the red Titan Tholins (Khare and Sagan 1984) resided between  $\sim 1400$  K and  $\sim 1800$  K in Gl 229B’s atmosphere. Indeed, TiO does give roughly the correct continuum slope, but it imposes the characteristic TiO bands on the spectrum that are not seen in either late L or T dwarfs. Furthermore, chemical abundance studies show that Ti and V are depleted (rained out) from the atmosphere to depths below the silicate clouds and to temperatures near 2000 K, far below the Gl 229B’s visible atmosphere. As to the suggestion by Griffith *et al.*, the dependence on wavelength between  $0.85 \mu\text{m}$  and  $0.93 \mu\text{m}$  of the imaginary index of refraction of the hazes inferred by construction was  $\sim 5\times$  steeper than the corresponding published Tholin or polyacetylene values. Moreover, though Gl 229B has in its primary, Gliese 229A, a nearby source of UV photons needed to generate a haze, the late L dwarfs and the new field methane dwarfs do not, yet they demonstrate similar profound absorption in the blue.

## 2. The Pivotal Role of the K I Resonance Doublet at $\sim 7700 \text{ \AA}$

What motivated Griffith *et al.* to posit the presence of a photochemical haze was the need for a continuum absorber to suppress the “blue” flux and to act shortward of  $\sim 1.0 \mu\text{m}$  down to at least  $0.8 \mu\text{m}$  (Figure 1). Small Mie scattering particles might quite naturally have fit the bill. However, there is another, ready-made, source of continuum opacity, the red wings of the K I resonance lines at  $7665 \text{ \AA}$  and  $7699 \text{ \AA}$ , that are in just the right place, shortward of the Gl 229B data, with what appear to be just the right strength and opacity slope, to fully explain the anomalous data. The K I resonance doublet, due to the  $4s^2 S_{1/2} - 4p^2 P_{1/2,3/2}$  transitions, comes into its own only if other sources of opacity that dominate in M dwarfs, such as TiO and VO, are absent. The formation of refractories and their subsequent rainout accomplishes just that.

The concept of “rainout” warrants further explanation: When condensates form, there are two possible general categories for their ultimate distribution within an atmosphere. The condensate (solid grain or liquid drop) can remain well-mixed with the atmosphere above the condensation level, or the condensate can rain out of the atmosphere. In the latter case, the exact vertical profile of the condensate depends upon poorly understood microphysical processes. However, guided by experience with planetary atmospheres, we expect the condensate to form a cloud layer of some finite thickness. Both the condensable gas and its condensate are thus depleted above the cloud top. We refer to this process as “rainout.” In the other, well-mixed, case the condensate can continue to react with the gas; we refer to this case as complete thermochemical equilibrium. Based on the Gliese 229B data, on experience with the planets of our solar system, and on general physical grounds, some form of rainout seems to occur.

As shown by Burrows and Sharp (1999), Fegley and Lodders (1996), and Lodders (1999),

the alkali metals are less refractory than Ti, V, Ca, Al, Fe, and Mg and survive in abundance as neutral atoms in substellar atmospheres to temperatures of 1000 K to 1500 K. This is below the 1500 K to 2500 K temperature range in which the silicates, iron, the titanates, corundum, and spinel, etc. condense. Hence, in the depleted atmospheres of cool brown dwarfs alkali metals quite naturally come into their own. Figures 2 and 3 show some representative abundance profiles for the alkali metals Li, Cs, K, and Na, with and without rainout. A  $T_{\text{eff}} = 950$  K and  $g = 10^5$  cm s $^{-2}$  Gl 229B atmosphere model from Burrows *et al.* (1997) and Burrows and Sharp (1999) was used. As demonstrated in Figures 2 and 3, with or without rainout elemental potassium and sodium persist to low temperatures to near the top of the T dwarf atmosphere. However, the distributions of the atomic alkalis are not the same, with Li and Cs being deeper than Na and K. At lower temperatures in an atmosphere, the atomic forms give way to the chlorides and hydroxides (*e.g.*, LiOH). With rainout (Figure 2), below  $\sim 1000$  K both sodium and potassium exist as sulfides (Na<sub>2</sub>S and K<sub>2</sub>S) (Lodders 1999). Without rainout (Figure 3), a situation we deem unlikely, complete chemical equilibrium at low temperatures requires that sodium and potassium reside in the feldspars, high albite and sanidine. If such compounds formed and persisted at altitude, then the nascent alkali metals would be less visible, particularly in T dwarfs. For either case, as Figures 2 and 3 demonstrate, all the elemental alkalis reside in the lower-pressure/lower-temperature reaches of cool, substellar atmospheres.

Lines of Cs I at 8521 Å and 8943 Å, Rb I at 7800 Å and 7948 Å, Li I at 6708 Å, and Na I at 8183/8195 Å have already been identified in L dwarf spectra. In addition, as Figure 4 and Kirkpatrick *et al.* (1999) demonstrate, the K I doublet is clearly dominant in the spectra of such late L dwarfs as 2MASS-1228, 2MASS-0850, Denis-0205, and 2MASS-1632. Therefore, it is quite natural to explain the steep red slope of the new T dwarfs as being caused by the red wing of a saturated and pressure-broadened K I feature. This is the thesis of our paper. Moreover, Gl 229B's *I* band flux ( $M_I \sim 20.76$ ), as measured using WFPC2 on HST (Golimowski *et al.* 1998) can be explained by the same K I resonance feature and the Gl 229B *R* band flux ( $M_R \sim 24.0$ ), also measured by Golimowski *et al.* (1998), can be explained by a mix of the sodium D lines at 5890 Å, the lithium line at 6708 Å, and the blue tail of the K I resonance doublet. Note that the 1.25  $\mu\text{m}$  lines of excited K I have also been identified in T dwarfs (Strauss *et al.* 1999; Tsvetanov *et al.* 1999), so that the presence of potassium, at least at the higher temperatures in their atmospheres, is in no doubt. The alkali metal lines may well prove to be the key to probing the atmospheric structure of the methane dwarfs, since their distributions and relative depths (*cf.*, Figure 2) will be reflected in the systematic dependence of T and L dwarf spectra with  $T_{\text{eff}}$  and  $g$ .

### 3. Profiles of the Alkali Metal Resonance Lines

Before we proceed with a discussion of our synthetic Gl 229B spectra between 0.3  $\mu\text{m}$  and 1.5  $\mu\text{m}$  we discuss our algorithm for handling the pressure broadening of the alkali metal lines by molecular hydrogen. The line lists containing the wavelength of the transition, the lower

excitation energy, the  $\log(gf)$  value, and the quantum numbers of the participating states were obtained from the Vienna Atomic Line Data Base (Piskunov *et al.* 1995). The major transitions of immediate relevance are those that correspond to the Na D lines at 5890 Å and the K I resonance lines at 7700 Å. Given the high H<sub>2</sub> densities in brown dwarf atmospheres, the natural widths (for Na D,  $\sim 0.12$  mÅ) and Doppler widths of these lines are completely overwhelmed by collisional broadening. However, in general the line shapes are determined by the radial dependence of the difference of the perturber/atom potentials for the lower and upper atomic states (Griem 1964; Breene 1957, 1981) and these are rarely known. The line cores are determined by distant encounters and are frequently handled by assuming a van der Waals interaction potential with an adiabatic impact theory (Weisskopf 1933; Ch'en and Takeo 1957; Dimitrijević and Peach 1990) and the line wings are determined by close encounters and are frequently handled with a statistical theory (Holtzmark 1925; Holstein 1950). The transition between the two regimes is near the frequency shift ( $\Delta\nu$ ), or detuning, associated with the perturbation at the so-called Weisskopf radius ( $\rho_w$ ), from which the collision cross section employed in the impact theory is derived (Spitzer 1940; Anderson 1950). In the simple impact theory, the line core is Lorentzian, with a half width determined by the effective collision frequency, itself the product of the perturber density, the average relative velocity of the atom and the perturber ( $v$ ), and the collision cross section ( $\pi\rho_w^2$ ). If the frequency shift ( $\Delta\nu$ ) due to a single perturber is given by  $C_n/r^n$ , where  $r$  is the interparticle distance, then  $\rho_w$  is determined from the condition that the adiabatic phase shift,  $\int_{-\infty}^{\infty} 2\pi\Delta\nu dt$ , along a classical straight-line trajectory, with an impact parameter  $\rho_w$ , is of order unity. This yields  $\rho_w \propto (C_n/v)^{1/(n-1)}$ . For a van der Waals force,  $n = 6$ . In the statistical theory, the line shape is a power law that goes like  $1/\Delta\nu^{\frac{n+3}{n}}$ , and this is truncated (cut off) by an exponential Boltzmann factor,  $e^{-V_0(r_s)/kT}$ , where  $V_0(r_s)$  is the ground-state perturbation at the given detuning. The detuning at the transition between the impact and statistical regimes is proportional to  $(v^6/C_n)^{0.2}$  (Holstein 1950).

All this would be academic, were it not that for the Na/H<sub>2</sub> pair the simple theory in the core and on the red wing is a good approximation (Nefedov, Sinel'shchikov, and Usachev 1999). We use this theory here. For the Na D lines perturbed by H<sub>2</sub>, we obtain from Nefedov, Sinel'shchikov, and Usachev (1999) a  $C_6$  of  $2.05 \times 10^{-32}$  cgs and a transition detuning, in inverse centimeters, of  $30 \text{ cm}^{-1}(T/500K)^{0.6}$ , where  $T$  is the temperature. For the K I resonance lines, we scale from the Na D line data, using a  $C_6$  of  $1.16 \times 10^{-31}$  cgs, itself obtained from the theory of Unsöld (1955). This procedure yields a transition detuning for the 7700 Å doublet of  $20 \text{ cm}^{-1}(T/500K)^{0.6}$ . From Nefedov, Sinel'shchikov, and Usachev (1999), we see that for a variety of perturbing gases the exponential cutoff for the Na D lines can be (for temperatures of 1000–2000 K) a few  $\times 10^3$  cm<sup>-1</sup>. The difference between 5890 Å and 7700 Å, in inverse wavenumbers, is  $\sim 4000 \text{ cm}^{-1}$  and that between 7700 Å and 1.0 μm is only 3000 cm<sup>-1</sup>. Hence, it is reasonable to expect that the detunings at which the line profiles are cut off can be much larger than the Lorentzian widths or the impact/statistical transition detunings of tens of cm<sup>-1</sup>. Since we as yet have no good formula for the exponential cutoff term, we assume that it is of the form  $e^{-qh\Delta\nu/kT}$ , where  $q$  is an unknown parameter. Comparing with the examples in Nefedov, Sinel'shchikov, and Usachev (1999),  $q$  may

be of order 0.3 to 1.0 for the Na/H<sub>2</sub> pair. Without further information or guidance, we assume that it is similar for the K/H<sub>2</sub> pair. We stress that this algorithm is merely an ansatz and that a more comprehensive theory based on the true perturber potentials is sorely needed. Nevertheless, whatever the detailed line shape, as we will show, the basic conclusion that the K I resonance doublet is the “mystery” absorber in the near-infrared spectra of T dwarfs seems robust.

Figure 5 depicts our opacity spectrum versus wavelength for the K I doublet at  $T = 2000$  K and 1 bar pressure, for three different parameterizations. Included are other, non-resonant, potassium lines excited by the high temperature. The solid line is for the standard Lorentzian theory, without a transition to the 3/2-power law. The other lines depict the line profile, corrected in the wings and with an exponential cutoff, using either  $q = 1.0$  or  $q = 0.5$ . Note that for  $q = 1.0$ , beyond the core the transition to the 3/2-power law from the Lorentzian “2”-power law results in a larger opacity, which is then brought below the Lorentzian profile by the exponential. The same behavior is seen for  $q = 0.5$ , but the exponential brings the profile below the Lorentzian at a larger detuning. In all cases, the slope redward of the 7700 Å doublet between 0.8  $\mu\text{m}$  and 1.0  $\mu\text{m}$  is of just the sort to affect the desired reddening.

#### 4. Model Spectra for Gliese 229B

Gliese 229B has been well-studied from the red to  $\sim 10$   $\mu\text{m}$  and has a well-measured distance (5.8 parsecs). Hence, with moderate resolution spectra in hand and absolute fluxes it is natural to use Gl 229B to demonstrate our basic thesis about the near-infrared and optical spectra of the entire T dwarf class. On Figure 1, in addition to depicting the “Clear” atmosphere fluxes from 0.5  $\mu\text{m}$  to  $\sim 1.45$   $\mu\text{m}$ , we give the synthetic spectra for four different models of Gl 229B that include the lines of the alkali metal atoms, in particular the K I doublet at 7700 Å, employing the formalism of §3. The Gl 229B data are taken from Leggett *et al.* (1999). Rainout abundance profiles of the alkali metals were used (*cf.*, Figure 2). As Figure 1 demonstrates, the fit between 0.85  $\mu\text{m}$  and 1.0  $\mu\text{m}$  is quite good and does not seem to require a layer of red particulates. We were guided in our choices of  $T_{\text{eff}}$ , gravities, and metallicities for these models by the work of Marley *et al.* (1996), Allard *et al.* (1996), and Griffith *et al.* (1998). Three of the models, those with higher fluxes around 0.7  $\mu\text{m}$  and lower fluxes near 1.0  $\mu\text{m}$  used a  $q$  of 0.4 and assumed alkali metal abundances of 0.3 times solar (Anders and Grevesse 1989). They had  $T_{\text{eff}}/g$  pairs of [900 K/10<sup>5</sup> (cgs)], [950 K/10<sup>5</sup> (cgs)], and [800 K/3 × 10<sup>4</sup> (cgs)]. From Burrows *et al.* (1997), the ages and masses for these models are 1.46 Gyr/34.9  $M_{\odot}$ , 1.26 Gyr/35.3  $M_{\odot}$ , and 0.44 Gyr/14.8  $M_{\odot}$ , respectively. The fourth model, that with the lowest fluxes near 0.7  $\mu\text{m}$  and the highest fluxes near 1.0  $\mu\text{m}$ , employed a  $q$  of 1.0, had a  $T_{\text{eff}}/g$  pair of [950 K/10<sup>5</sup> (cgs)], and assumed that the alkali metal abundances were solar.

Figure 6 depicts the behavior of the theoretical spectra as a function of  $q$ , from 0 to 1, for the [950 K/10<sup>5</sup> (cgs)] model (with 0.3×solar alkali metal abundances). Also included is the predicted spectrum for the uncorrected Lorentzian K I line profile (dotted). Though Figure 6 depicts a

range of near-infrared and optical spectra, the character of these spectra is similar. However, as a consequence of the current ambiguity in the proper shape of the 7700 Å profile, which we have parameterized with  $q$ , we can not yet tie down the alkali metal abundances to better than perhaps a factor of three. Nevertheless, the good fits indicated in Figure 1 are quite compelling. Rather stunningly, both the measured WFPC2  $I$  band flux near 0.814  $\mu\text{m}$  and the WFPC2  $R$  flux near 0.675  $\mu\text{m}$  (Golimowski *et al.* 1998) fit as well. Hence, we conclude that the  $I$  band flux is determined by the red wing of the K I resonance doublet and that the  $R$  band is a consequence of the red wings of the Na D lines ( $\sim 5890$  Å), the blue wings of the K I doublet, and, perhaps, the lithium line at 6708 Å. The broad width of the  $I$  band filter extends it to beyond the saturated center of the doublet at 7700 Å. Our theoretical models have absolute  $I$  band magnitudes from 21.0 to 21.3, compared with the measured value of  $\sim 20.76$ . Given the calibration problems when an underlying spectral slope is so steep and so unlike that of the standard stars, we conclude that the fit is indeed good. As Figure 1 demonstrates, our  $R$  band predictions bracket the  $R$  band measurement.

We note in passing that the discrepancy between the depth of the predicted and measured flux trough between the  $Z$  ( $\sim 1.05$   $\mu\text{m}$ ) and the  $J$  ( $\sim 1.25$   $\mu\text{m}$ ) bands may be resolved with a lower abundance of water and, hence, oxygen (Griffith *et al.* 1998) and that the shape of the  $J$  band can not be fit without the methane bands at  $\sim 1.15 - 1.2$   $\mu\text{m}$  and  $\sim 1.3$   $\mu\text{m}$  to sculpt it. Hence, the shape of the  $J$  band in T dwarfs is not just a consequence of bracketing by  $\text{H}_2\text{O}$  absorption features, but requires methane and is another signature of methane in their atmospheres. However, this point, as well as the inferred elemental abundances, are not the subject of the current paper and we defer a fuller discussion to a later work.

The variety of models that fit the Gl 229B data, given the current state of the theory and observations, was noted in Marley *et al.* (1996) and Allard *et al.* (1996) and reflects the fact that different models with different  $T_{\text{eff}}/g$  pairs can have similar atmospheric temperature–pressure profiles and luminosities. The atmospheres of substellar objects are convective at depth and radiative on the periphery. For a given composition, brown dwarfs and extrasolar giant planets (EGPs; Burrows *et al.* 1995) are a two-parameter family; given two independent quantities such as  $T_{\text{eff}}$ , luminosity, radius, gravity, or age, one can derive, with theory, any of the others. In particular, as discussed in Hubbard (1977) and Saumon *et al.* (1996), in an approximate sense, the entropy ( $S$ ) at depth is a function of  $T_{\text{eff}}$  and  $g$  and this entropy determines the temperature/pressure profile. (This is not to say that the atmospheres are adiabatic, merely that the T/P profile of the outer radiative zone can be calculated from  $S$ ,  $T_{\text{eff}}$ , and  $g$ .) Hubbard (1977) showed that  $S$  is approximately a function of the combination  $T_{\text{eff}}^{0.95}/g^{1/6}$ . From Marley *et al.* (1996), we obtain rough power-law relations for mass ( $M$ ), radius ( $R$ ), and age ( $t$ ), as a function of  $g$  and  $T_{\text{eff}}$ :

$$\begin{aligned} M &= 35M_{\text{J}} \left( \frac{g}{10^5} \right)^{0.64} \left( \frac{T_{\text{eff}}}{10^3} \right)^{0.23} \\ R &= 6.7 \times 10^4 \text{ km} \left( \frac{10^5}{g} \right)^{0.18} \left( \frac{T_{\text{eff}}}{10^3} \right)^{0.11} \end{aligned}$$

$$t = 1.1 \text{Gyr} \left( \frac{g}{10^5} \right)^{1.7} \left( \frac{10^3}{T_{\text{eff}}} \right)^{2.8}, \quad (1)$$

where  $g$  is in  $\text{cm s}^{-2}$ . From these equations, and the dependence of  $S$  on  $T_{\text{eff}}$  and  $g$  cited above, we derive approximately that, for a given core entropy and, hence, for a given T/P profile,  $M \sim t^{0.55}$ . Using the same set of power laws, we can derive that, for a given luminosity,  $M \sim t^{0.43}$ . Hence, since these two power-law relations are similar, fits to Gl 229B roughly define a trajectory in  $M$ - $t$  space with a  $\sim 0.5$  power. This is why low-mass/short-age models and high-mass/long-age models both fit Gl 229B, at least for the low-resolution comparisons thus far attempted. In principle, this degeneracy can be broken once the theory and the observations are better constrained. Figure 7 shows temperature/pressure profiles for a few models from Burrows *et al.* (1997). The higher curves are for higher  $T_{\text{eff}}$ s and lower gravities. Note that the lower- $T_{\text{eff}}$ , lower- $g$  model [800 K/3  $\times 10^4$  (cgs)] is in the same vicinity as the higher- $T_{\text{eff}}$ , higher- $g$  model [900 K/10 $^5$  (cgs)], both of which are good fits to Gl 229 B (Figure 1). Note also that the [1100 K/5  $\times 10^4$  (cgs)], [400 K/5  $\times 10^4$  (cgs)], and [800 K/10 $^5$  (cgs)] models depicted for comparison do not fit Gl 229B, as we might have surmised from Figure 7.

## 5. The Sloan Dwarf: SDSS 1624+00

The models and data depicted in Figure 1 capture the Cs lines at 8521 Å and 8943 Å, indicating that cesium is in Gl 229 B’s atmosphere in modest abundance between 1200 K and 1400 K. The depths to which cesium can be found are shown in detail for a specific model in Figures 2 and 3 and approximately for the variety of models by the position of the intercept in Figure 7 of the “Cs/CsCl=1” line with a given T/P profile. Similarly, the depths of atomic K, Na, Rb, and Li can be found. Shown on Figure 7 along with the Cs/CsCl=1 line is a corresponding complete equilibrium (no rainout) “K/KCl=1” trajectory. As Figure 2 demonstrates, with rainout (a more realistic situation), atomic potassium persists to much lower temperatures, perhaps shifting the K/KCl=1 line on Figure 7 down by 200–300 K. Nevertheless, qualitatively and importantly, the lower the T/P profile in Figure 7, the deeper are the atomic cesium and potassium. Depth and higher pressure imply a higher column density of H<sub>2</sub>O, CH<sub>4</sub>, and H<sub>2</sub> and, hence, a higher optical depth of these competing absorbers. Therefore, for a given composition, at lower  $T_{\text{eff}}$  and higher  $g$ , both potassium and cesium are more deeply buried than at higher  $T_{\text{eff}}$  and lower  $g$ . The expected upshot is the gradual diminution with decreasing core entropy of the strengths of the cesium and potassium features. A decrease in the effect of the K I resonance doublet at 7700 Å would result in an increase in the influence below 1.0  $\mu\text{m}$  of the H<sub>2</sub>O, CH<sub>4</sub>, and H<sub>2</sub> features that are not as steep as the red wing of the doublet. As a result, the spectrum short of  $\sim 0.95$   $\mu\text{m}$  would shallow and the 7700 Å region of the spectrum would fill in. The Rb lines at 7800 Å and 7948 Å may make an appearance in the K I trough, but they will still be rather weak. Note that, for a given  $T_{\text{eff}}/g$  pair, lowering the abundances of the alkali metals would raise the flux in the 0.7–0.95  $\mu\text{m}$  region, but it might also make the  $Z - J$  color bluer than observed for the current crop of T dwarfs. Furthermore, the presence of the potassium line at 1.25  $\mu\text{m}$  both in Gl 229B and in the two Sloan

dwarfs makes this explanation suboptimal. Nevertheless, potential variations in abundances and metallicity from object to object do complicate the analysis.

The shallowing of the spectrum shortward of  $0.9 \mu\text{m}$  and the weakening of the cesium features at  $8521 \text{ \AA}$  and  $8943 \text{ \AA}$  are indeed seen in the spectrum of SDSS 1624+00 (Strauss *et al.* 1999). Strauss *et al.* note that the spectra of Gl 229B and SDSS 1624+00 seem uncannily similar and conclude that they must have similar mass, age, and  $T_{\text{eff}}$ . Given the lower apparent flux of SDSS 1624+00, they put this object further away than Gl 229B, at  $\sim 10$  parsecs. However, theory implies the  $J - H$  and  $J - K$  colors don't change hugely in the  $600 \text{ K}$  to  $1100 \text{ K}$  range (Burrows *et al.* 1997). As a consequence, for a given gravity or mass, a decrease in  $T_{\text{eff}}$  merely, though approximately, translates the absolute spectrum down to lower fluxes. Hence, there is a need for more subtle diagnostics of a substellar object's properties. Such diagnostics may be the strengths of the alkali metal lines in the optical and near infrared. Figure 8 compares the observed SDSS 1624+00 spectrum with a theoretical model spectrum, as well as with the observed Gl 229B spectrum. The model (dotted) has an atmosphere with  $T_{\text{eff}} = 700 \text{ K}$  and  $g = 3 \times 10^4 \text{ cm s}^{-2}$ . Its core entropy is below those of the Gl 229B models. We theorize that the shallower near-infrared spectrum of SDSS 1624+00 with respect to Gl 229B, as well as the weakness of the Cs lines, are both consequences of a lower core entropy T/P profile. This could mean a lower  $T_{\text{eff}}$ , a higher  $g$  or mass, or some suitable combination that buries the tops of the potassium and cesium distributions at higher pressure and, hence, larger  $\text{H}_2\text{O}$  optical depths than found in Gl 229B. However, given the remaining theoretical ambiguities, we can't completely rule out the possibility that lower K and Cs abundances are the explanation. Note that it is very possible that  $T_{\text{eff}}$  for SDSS 1624+00 is larger than  $700 \text{ K}$ . However, we would then require its gravity, and presumably its mass, to be correspondingly higher to achieve the lower core entropy we suggest can explain its spectrum. Note also that with the  $[700 \text{ K}/3 \times 10^4 \text{ cgs}]$  model, the absolute  $Z$  and  $J$  band fluxes of the SDSS 1624+00 are below those for Gl 229B and match only near  $\lambda = 0.85 \mu\text{m}$ . If the  $T_{\text{eff}}$  of SDSS 1624+00 is indeed lower than that of Gl 229B, SDSS 1624+00 could be closer than the 5.8 parsecs of Gl 229B. Hence, obtaining a parallax for this new T dwarf will be a crucial prerequisite for future substantial improvements in characterizing it.

For a given mass and composition, the “history” of the alkali metal lines in L and T dwarfs may follow the following sequence: At higher  $T_{\text{effs}}$  (in the L dwarf range), the depletion of the refractory elements allows the strengths of the alkali metal lines to wax. The cesium lines peak before reaching the  $T_{\text{eff}}$  of Gl 229B, though they are still prevalent in such atmospheres, and potassium determines the character of the spectrum from  $0.7 \mu\text{m}$  through  $1.0 \mu\text{m}$ . As  $T_{\text{eff}}$  decreases further, the alkali metals are buried progressively more deeply and begin to wane in strength. Due to this burial of potassium, the slope of the spectrum from  $0.8 \mu\text{m}$  to  $1.0 \mu\text{m}$  decreases. Since the abundance distribution of the atomic form of each alkali metal is different (Figures 2 and 3), the  $T_{\text{effs}}$  at which the lines of a given alkali start to wane will be different, with the effects of Li, Cs, Rb, K, and Na waning in approximately that order with decreasing  $T_{\text{eff}}$  (at a given mass and metallicity). The specific numbers will depend upon the actual effects of rainout on the alkali

metal profiles, but the systematics should not. Eventually, perhaps below  $T_{\text{eff}}$ s of 500–600 K, the effects of the neutral alkali metals are eclipsed, with clouds of  $\text{H}_2\text{O}$  eventually effecting the next important change in the character of brown dwarf atmospheres.

## 6. Summary

We conclude that the anomalous absorption seen in the near-infrared and optical spectra of all the T dwarfs discovered to date is due to the red wings of the saturated K I resonance lines at 7700 Å. This theory also explains the WFPC2 *I* and *R* flux measurements made of Gl 229B, with the Na D lines at 5890 Å helping to determine the strength of the *R* band. There are still ambiguities in the  $T_{\text{eff}}$ s, gravities, and compositions of Gl 229 B, in particular, and of T dwarfs, in general, but a sequence from Gl 229B to SDSS 1624+00 of decreasing core entropy is seen to be consistent with the expected systematics of the temperature/pressure and alkali–metal abundance profiles. (However, lower K and Cs abundances for the Sloan dwarf can not yet be ruled out.) Silicate grains are expected at depths of 1500 K to 2500 K. Their formation is inferred in the late M dwarfs (Jones and Tsuji 1997) and their eventual burial is seen in the appearance at lower  $T_{\text{eff}}$ s of the new L spectral class (Kirkpatrick *et al.* 1999). Complete refractory element depletion ushers in a phase of neutral alkali metal dominance at short wavelengths, which persists until the tops of the alkali metal distributions are buried at higher pressures and higher  $\text{H}_2\text{O}$ ,  $\text{CH}_4$ , and  $\text{H}_2$  optical depths. This occurs in low–entropy atmospheres, though low alkali metal abundances can mimic the same effect somewhat. We note that if the Lorentzian theory for the line shapes of the Na D lines were used, due to the high relative abundance of sodium, their influence would stretch 7000  $\text{cm}^{-1}$  to 1.0  $\mu\text{m}$  and would flatten the top of the *Z* band, contrary to observation. This is indirect evidence for the action of an “exponential cutoff” on the Na D line shape. Even with such a cutoff, the K I resonance line dominates the spectra of Gl 229 B and its ilk from 0.7  $\mu\text{m}$  to 1.0  $\mu\text{m}$ . For Gl 229 B, we predict the presence of a saturated absorption line around 7700 Å, with higher fluxes on either side. We also expect a deep, broad trough around the Na D lines at 5890 Å (see Figure 1).

At the time of this writing, we became aware of a paper by Tsuji *et al.* (1999) that has also concluded that the K I feature is the major, “mystery” absorber at short wavelengths. We wholeheartedly concur with this conclusion. However, contrary to Tsuji *et al.*, we determine that dust may not be required to achieve a good fit shortward of 1.0  $\mu\text{m}$ . Moreover, we believe that the Gliese 229B *I* band flux is well–fit by the red wing of the K I doublet alone. In addition, if the Na D lines are included in a natural way, an acceptable fit to the WFPC2 *R* band flux is achieved as a byproduct. However, filling in the troughs between the *Z* and *J* bands and between the *H* and *K* bands may still require some combination of grains, as Tsuji *et al.* suggest, and sub–solar metallicity.

Note that in this paper we have considered only objects in isolation. However, we expect that those EGPs that achieve  $T_{\text{eff}}$ s in the 800–1300 K range due to stellar insolation will also show

signatures of the neutral alkali metals. Recently, Charbonneau *et al.* (1999) have put an upper limit of 0.3 to the geometric albedo at  $\lambda = 0.48 \mu\text{m}$  of the planet orbiting  $\tau$  Boo. This is below published predictions (Marley *et al.* 1999; Seager and Sasselov 1998) and may indicate the presence in its atmosphere of sodium and absorption by the Na D lines (Sudarsky, Burrows, and Pinto 1999). Our preliminary estimate of the geometric albedo at  $\lambda = 0.48 \mu\text{m}$  of such a planet, due to the influence of the neutral alkali metals, is  $< 0.1$ . Since stellar insolation is bound to create hazes (Marley 1998), such as absorb in the blue and UV in Jupiter, detailed reflection spectra of  $\tau$  Boo and similar “close-in” EGPs will be needed to disentangle the relative contribution of the alkali metals to EGP albedos.

We thank Richard Freedman, Phil Pinto, Dick Tipping, Jonathan Lunine, Bill Hubbard, David Sudarsky, Didier Saumon, Ben Oppenheimer, Sandy Leggett, and Jim Liebert for many useful contributions, as well as for good advice. This work was supported in part by NASA grants NAG5-7499, NAG5-7073, NAG2-6007, and NAG5-4987, as well as by an NSF CAREER grant (AST-9624878) to M.S.M.

## REFERENCES

Allard, F., Hauschildt, P.H., Baraffe, I. & Chabrier, G. 1996, ApJ, 465, L123  
Anders, E. & Grevesse, N. 1989, Geochim. Cosmochim. Acta, 53, 197  
Anderson, P.W. 1950, Phys. Rev., 79, 132  
Breene, R.G. Jr. 1957, Rev. Mod. Phys., 29, 94  
Breene, R.G., Jr. 1981, “Theories of Spectral Line Shape,” (New York: John Wiley), p. 344.  
Burgasser, A.J. *et al.* 1999, accepted to ApJ, astro-ph/9907019  
Burrows, A., Saumon, D., Guillot, T., Hubbard, W.B., & Lunine, J.I. 1995, Nature, 375, 299  
Burrows, A., Marley M., Hubbard, W.B. Lunine, J.I., Guillot, T., Saumon, D. Freedman, R., Sudarsky, D. & Sharp, C.M. 1997, ApJ, 491, 856  
Burrows, A. and Sharp, C.M. 1999, ApJ, 512, 843  
Charbonneau, D. *et al.* 1999, accepted to ApJ  
Ch'en, S. and Takeo, M. 1957, Rev. Mod. Phys., 29, 20  
Delfosse, X., Tinney, C.G., Forveille, T., Epchtein, N., Bertin, E., Borsenberger, J., Copet, E., De Batz, B., Fouqué, P., Kimeswenger, S., Le Bertre, T., Lacombe, F., Rouan, D., & Tiphène, D. 1997, Astron. Astrophys. , 327, L25  
Cuby, J.G., Saracco, P., Moorwood, A.F.M., D'Odorico, S., Lidman, C., Comeron, F., and Spyromilio, J. 1999, astro-ph/9907028  
Dimitrijević, M.S. & Peach, G. 1990, A&A, 236, 261

Fegley, B. & Lodders, K. 1996, ApJ, 472, L37

Geballe, T.R., Kulkarni, S.R., Woodward, C.E., and Sloan, G.C. 1996, ApJ, 467, L101

Golimowski, D. A., *et al.* 1998, AJ, 115, 2579

Griem, H.R. 1964, “Plasma Spectroscopy,” (New York: McGraw Hill).

Griffith, C.A., Yelle, R.V., and Marley, M.S. 1998, Science, 282, 2063

Holstein, T. 1950, Phys. Rev., 79, 744

Holtzman, J. 1925, Z. für Physik, 34, 722

Hubbard, W. B. 1977, Icarus, 30, 305

Jones, H.R.A. & Tsuji, T. 1997, ApJ, 480, L39

Khare, B.N. and Sagan, C. 1984, Icarus, 60, 127

Kirkpatrick, J.D., Reid, I.N., Liebert, J., Cutri, R.M., Nelson, B., Beichman, C.A., Dahn, C.C., Monet, D.G., Gizis, J., and Skrutskie, M.F. 1999, ApJ, 519, 802

Leggett, S., Toomey, D.W., Geballe, T., and Brown, R.H. 1999, ApJ, in press

Lodders, K. 1999, ApJ, 519, 793

Marley, M.S., Saumon, D., Guillot, T., Freedman, R.S., Hubbard, W.B., Burrows, A. & Lunine, J.I. 1996, Science, 272, 1919

Marley, M.S. 1998, in the proceedings of the Tenerife Workshop on Extrasolar Planets and Brown Dwarfs, ed. R. Rebolo, E.L. Martin, & M.R. Zapatero–Osorio (ASP Conf. Series V. 134), p. 383.

Marley, M.S., Gelino, C., Stephens, D., Lunine, J.I., & Freedman, R. 1998, ApJ, 513, 879

Nakajima, T., Oppenheimer, B.R., Kulkarni, S.R., Golimowski, D.A., Matthews, K. & Durrance, S.T. 1995, Nature, 378, 463

Nefedov, A.P., Sinel’shchikov, V.A., and Usachev, A.D. Physica Scripta, 59, 432

Noll, K., Geballe, T.R., & Marley, M.S. 1997, ApJ, 489, 87

Oppenheimer, B.R., Kulkarni, S.R., Matthews, K., & Nakajima, T. 1995, Science, 270, 1478

Oppenheimer, B.R., Kulkarni, S.R., Matthews, K., & van Kerkwijk, M.H. 1998, ApJ, 502, 932

Piskunov, N.E., Kupka, F., Ryabchikova, T.A., Weiss, W.W., & Jeffery, C.S. 1995, A&ASuppl., 112, 525

Saumon, D., Hubbard, W.B., Burrows, A., Guillot, T., Lunine, J.I., & Chabrier, G. 1996, ApJ, 460, 993

Schultz, A.B. *et al.* 1998, ApJ, 492, L181

Seager, S. and Sasselov, D.D. 1998, ApJ, 502, L157

Spitzer, L., Jr. 1940, Phys. Rev., 58, 348

Strauss, M.A. *et al.* 1999, submitted to ApJ, astro-ph/9905391

Sudarsky, D., Burrows, A., and Pinto, P. 1999, in preparation

Tinney, C.G., Delfosse, X., Forveille, T. and Allard, F. 1998, A&A, 338, 1066

Tsuji, T., Ohnaka, K., Aoki, W., & Nakajima, T. 1996, Astron. Astrophys. , 308, L29

Tsuji, T., Ohnaka, K., and Aoki, W. 1999, ApJ, 520, L119

Tsvetanov, Z.I. *et al.* 1999, submitted to ApJ

Unsöld, A. 1955, “Physik der Sternatmosphären,” 2’nd edition (Berlin: Springer-Verlag), p. 305

Weisskopf, V. 1933, Z. für Physik, 43, 1

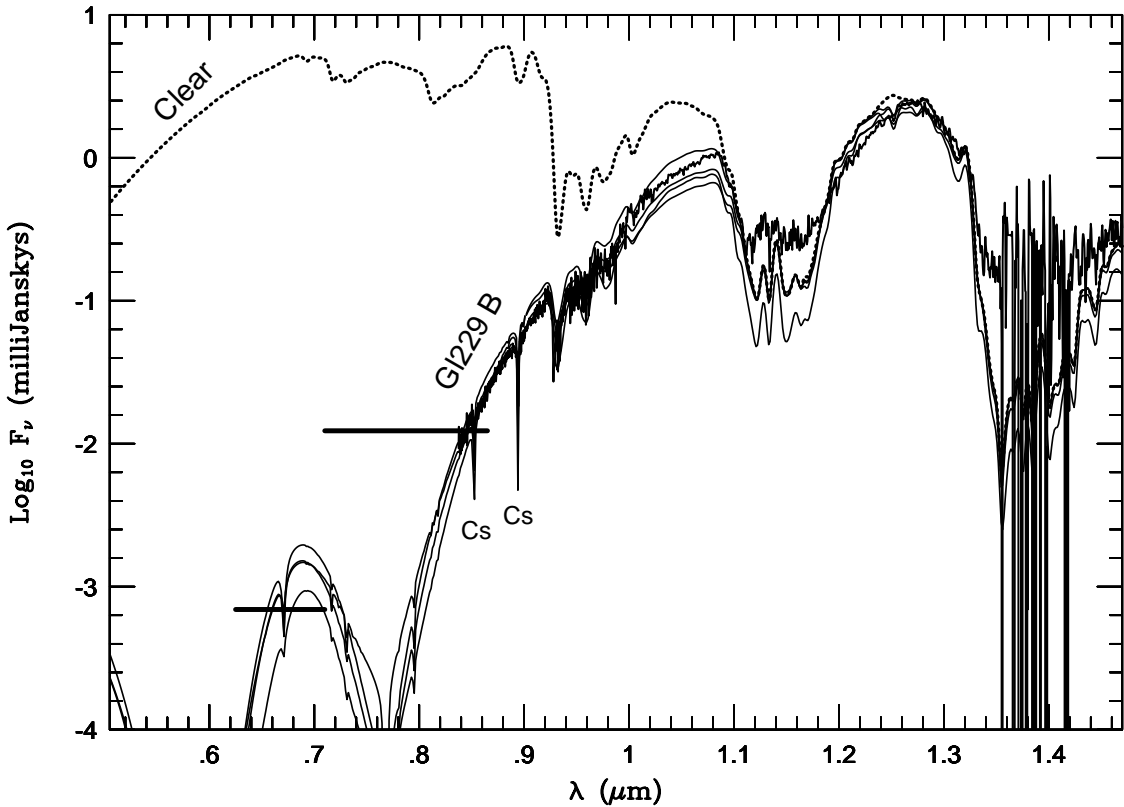


Fig. 1.— The log of the absolute flux ( $F_\nu$ ) in milliJanskys versus wavelength ( $\lambda$ ) in microns from  $0.5 \mu\text{m}$  to  $1.45 \mu\text{m}$  for Gliese 229 B, according to Leggett *et al.* (1999) (heavy solid), and for four theoretical models (light solid) described in the text. Also included is a model, denoted “Clear” (dotted), without alkali metals and without any ad hoc absorber due to grains or haze. The horizontal bars near  $0.7 \mu\text{m}$  and  $0.8 \mu\text{m}$  denote the WFPC2  $R$  and  $I$  band measurements of Golimowski *et al.* (1998).

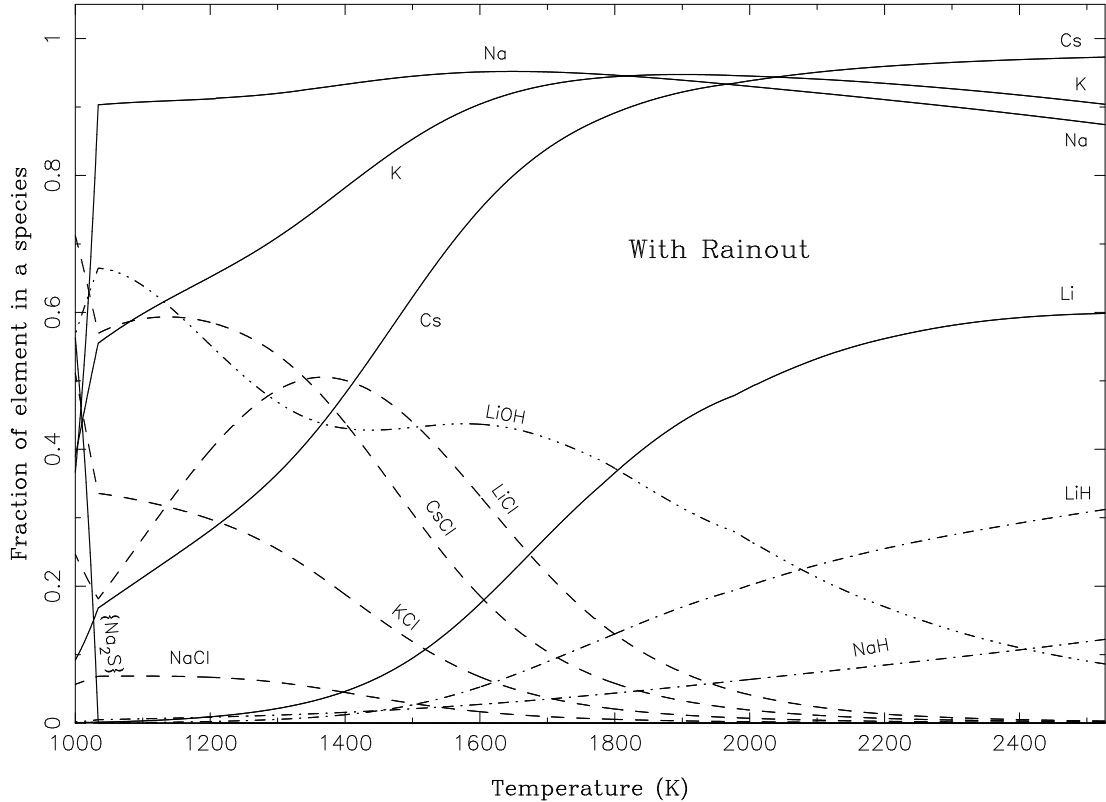


Fig. 2.— The fractional abundances of different chemical species involving the alkali elements Li, Na, K and Cs for a Gliese 229B model, with rainout as described in Burrows and Sharp (1999). The temperature/pressure profile for a  $T_{\text{eff}} = 950$  K and  $g = 10^5$  cm s $^{-2}$  model, taken from Burrows *et al.* (1997), was used. Each curve shows the fraction of the alkali element in the indicated form out of all species containing that element. All species are in the gas phase except for the condensates, which are in braces { and }. The solid curves indicate the monatomic gaseous species Li, Na, K and Cs, the dashed curves indicate the chlorides, the dot-dashed curves indicate the hydrides and the triple dot-dashed curve indicates LiOH. Due to rainout, at lower temperatures there is a dramatic difference with the no-rainout, complete equilibrium calculation (Figure 3); high albite and sanidine do not appear, but instead at a much lower temperature the condensate Na<sub>2</sub>S (disodium monosulfide) forms, as indicated by the solid line in the lower left of the figure. The potassium equivalent, K<sub>2</sub>S, also forms, but it does so below 1000 K and is not indicated here. The difference between this Figure and Figure 3 is that almost all the silicon and aluminum have been rained out at higher temperatures, so that no high albite and sanidine form at lower temperatures.

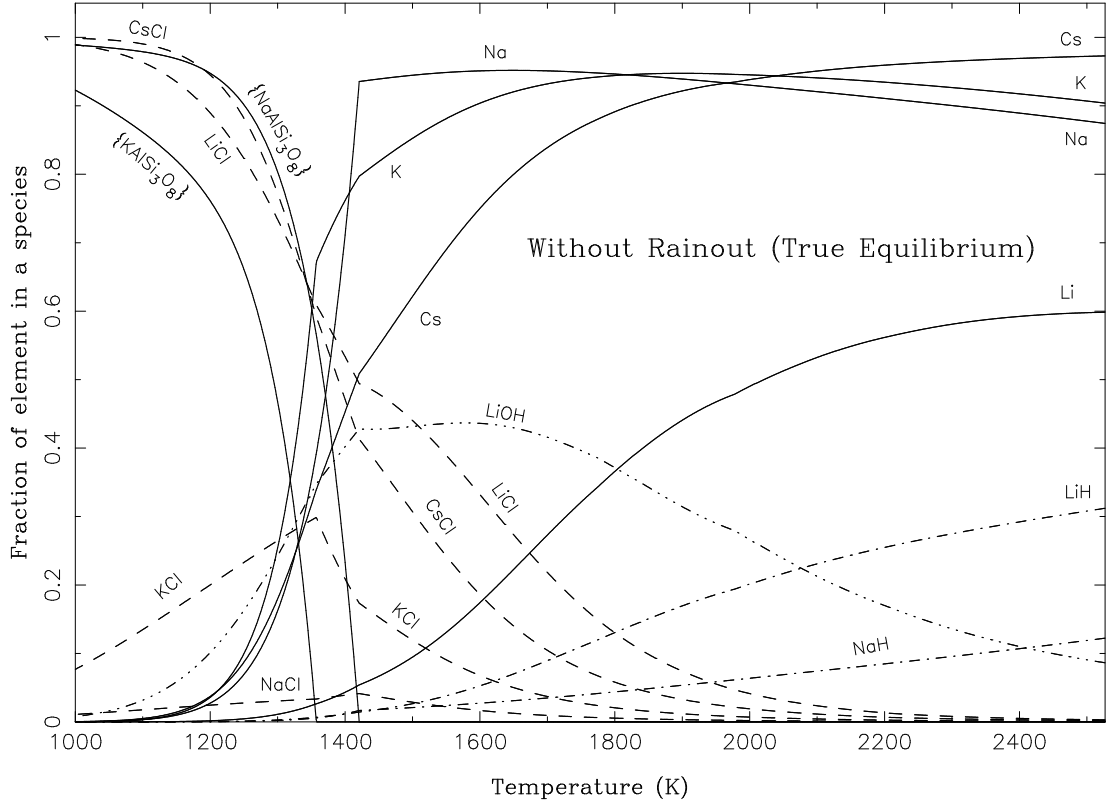


Fig. 3.— The fractional abundances of different chemical species involving the alkali elements Li, Na, K and Cs for a Gliese 229B model, assuming complete (true) chemical equilibrium and no rainout (disfavored). The temperature/pressure profile for a  $T_{\text{eff}} = 950$  K and  $g = 10^5$  cm  $s^{-2}$  model, taken from Burrows *et al.* (1997), was used. Each curve shows the fraction of the alkali element in the indicated form out of all species containing that element, *e.g.*, in the case of sodium, the curves labeled as Na, NaCl, NaH and NaAlSi<sub>3</sub>O<sub>8</sub> are the fractions of that element in the form of the monatomic gas and three of its compounds. All species are in the gas phase except for the condensates, which are in braces { and }. The solid curves indicate the monatomic gaseous species Li, Na, K and Cs and the two condensates NaAlSi<sub>3</sub>O<sub>8</sub> and KAlSi<sub>3</sub>O<sub>8</sub>, *i.e.*, high albite and sanidine, respectively, the dashed curves indicate the chlorides, the dot-dashed curves indicate the hydrides and the triple dot-dashed curve indicates LiOH.

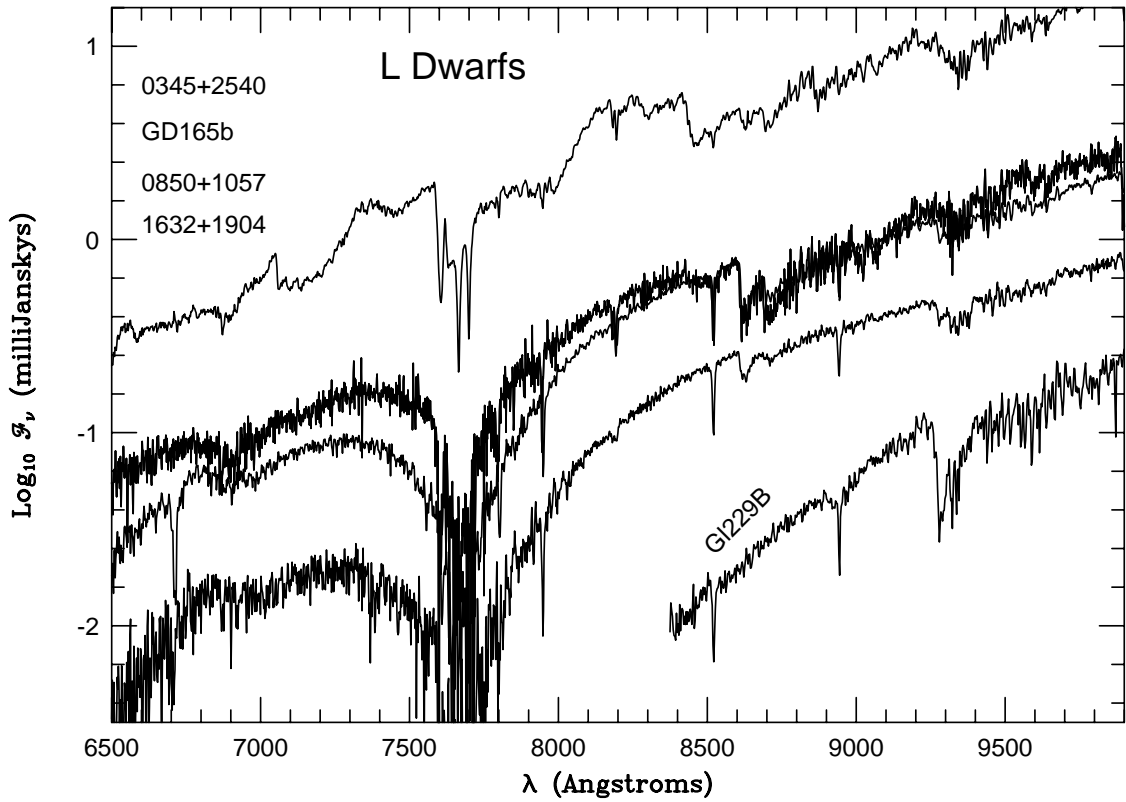


Fig. 4.— The log of the absolute flux ( $F_\nu$ ) in milliJanskys versus wavelength ( $\lambda$ ) in Å from 6500 Å to 10000 Å for Gliese 229 B and representative L dwarfs from Kirkpatrick *et al.* (1999). Included are 2MASP-J0345 (L0), GD 165b (L4), 2MASSs-J0850 (L6), and 2MASSW-J1632 (L8), in order of decreasing general flux level. The L dwarf spectra were put on an absolute scale using the distances and apparent  $I$  band magnitudes in Kirkpatrick *et al.* and should be used with extreme caution.

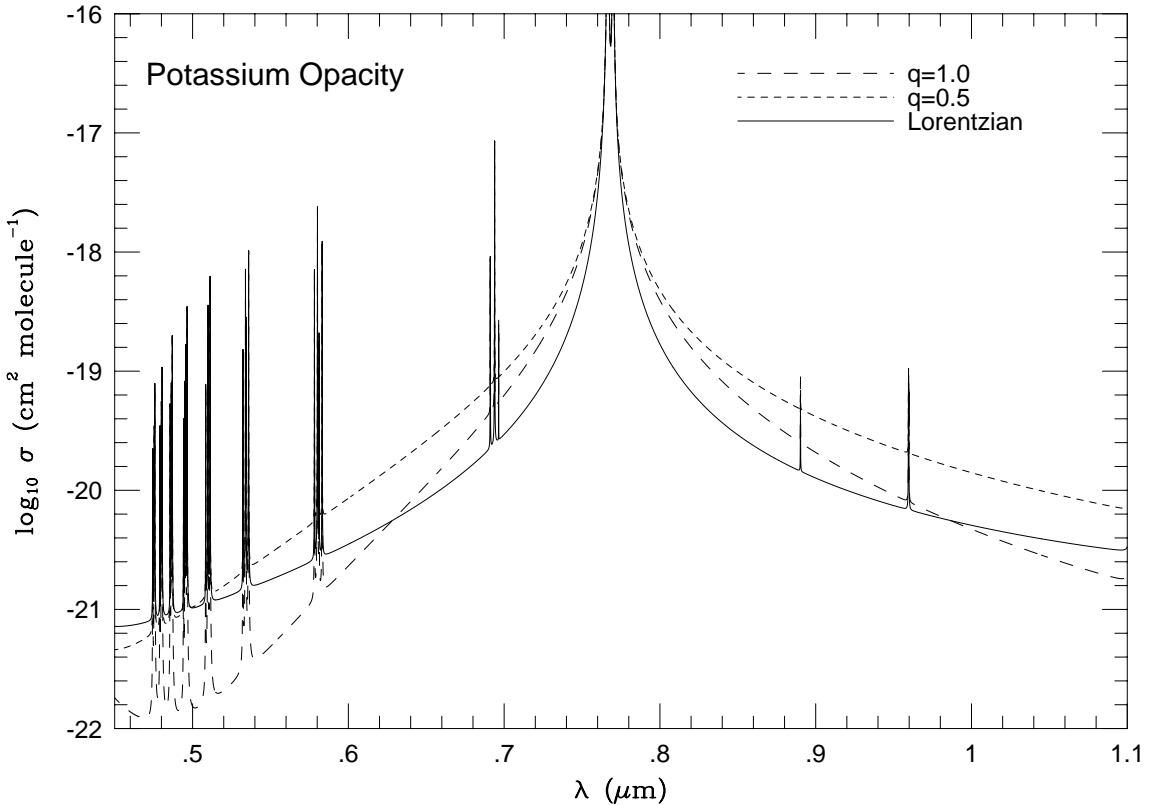


Fig. 5.— The log of the photon–potassium cross sections per particle, in  $\text{cm}^2$ , versus wavelength ( $\lambda$ ) in  $\mu\text{m}$ . The focus is on the region around the K I resonance doublet at  $7700 \text{ \AA}$  and for specificity a temperature and pressure of  $2000 \text{ K}$  and  $1 \text{ bar}$  have been assumed. The solid line is the Lorentzian theory without corrections in the broad wings at large detunings. The short-dashed and long-dashed lines are for the corrected theory, with  $q_s$  of  $0.5$  and  $1.0$ , respectively. The crucial fact is the useful slope between  $0.8 \mu\text{m}$  and  $1.0 \mu\text{m}$ .

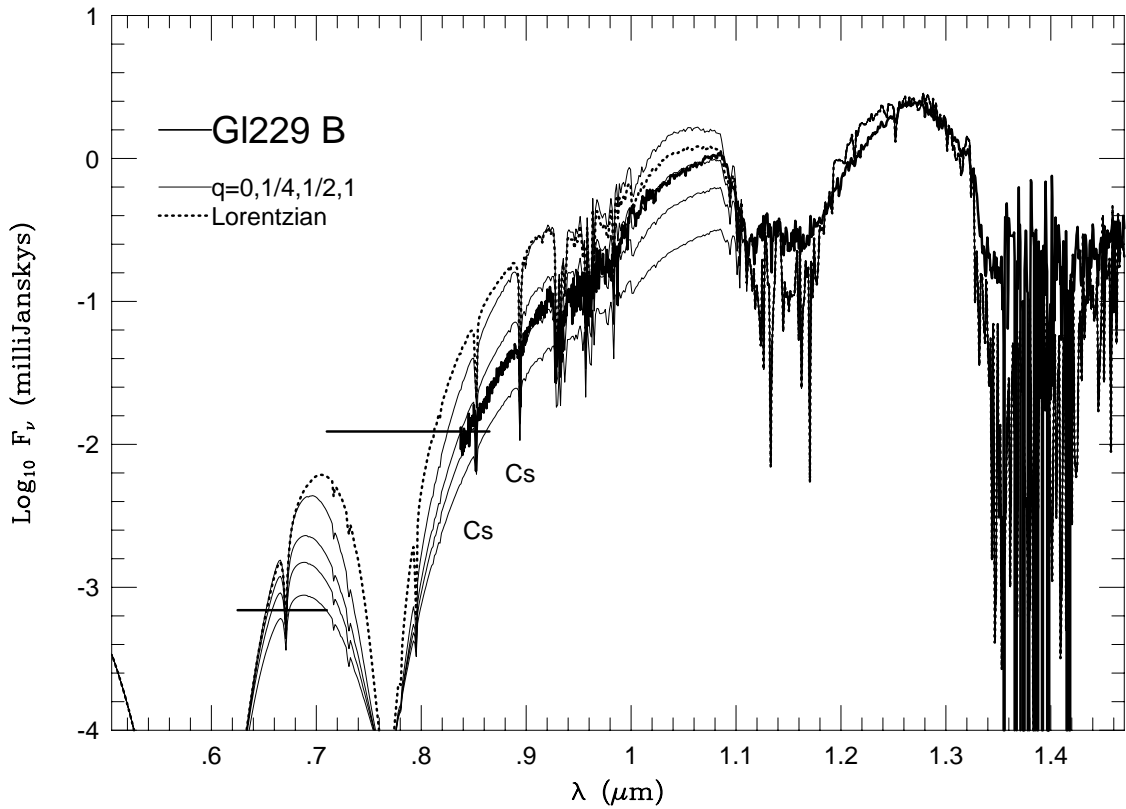


Fig. 6.— Similar to Figure 1, using the 950 K and  $g = 10^5$  cm s $^{-2}$  Gliese 229B model, but for  $qs$  of 0.0, 0.25, 0.5, and 1.0. The lower the  $q$ , the lower the curve. The dotted line is the theoretical spectrum using the Lorentzian profile. Alkali metal abundances of  $0.3 \times$  solar were assumed. The heavy solid line is the measured spectrum of Gliese 229B and the solid horizontal lines are the WFPC2 Gliese 229B  $R$  and  $I$  fluxes.

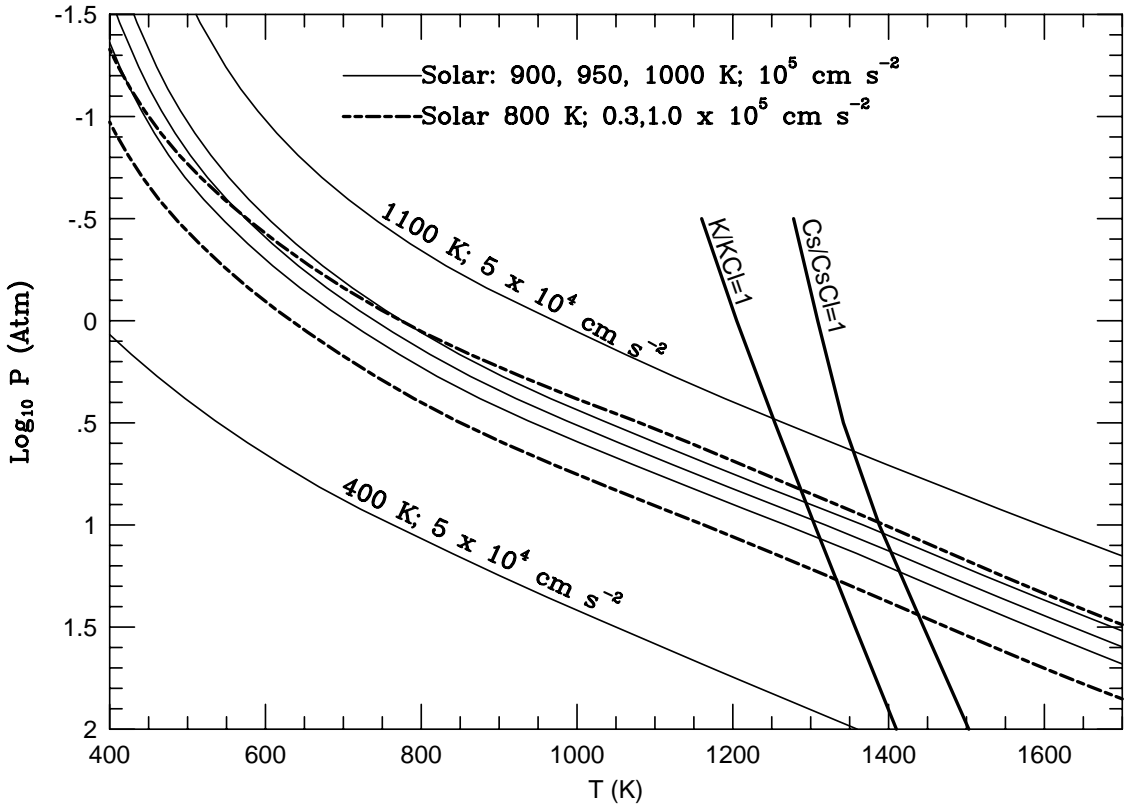


Fig. 7.— The pressure (in Atm) versus the temperature (in Kelvin) for various brown dwarf atmospheres, as a function of  $T_{\text{eff}}$  and gravity and at solar metallicity. The three central solid lines are for 900 K, 950 K, and 1000 K models with a gravity of  $10^5 \text{ cm s}^{-2}$ . The two outliers are models at temperatures (1100 K and 400 K) and entropies that are too high and too low, respectively, to fit the Gliese 229 B spectral data. The long-dash/short-dash curves are models with  $T_{\text{eff}} = 800 \text{ K}$ , the higher one at  $3 \times 10^4 \text{ cm s}^{-2}$  fits, while the lower one at  $10^5 \text{ cm s}^{-2}$  does not. Also included are the lines that demarcate the true-equilibrium, no-rainout temperature/pressure trajectories for which atomic K and gaseous KCl and atomic Cs and gaseous CsCl have equal abundances. While the Cs/CsCl line will be little changed by rainout, the K/KCl line will be shifted to lower temperatures by perhaps 200–300 K. These lines serve to indicate the character of the burial of the elemental alkali metals with decreasing core entropy. As the core entropy decreases, the pressures and column depths at the intersection points steadily increase.

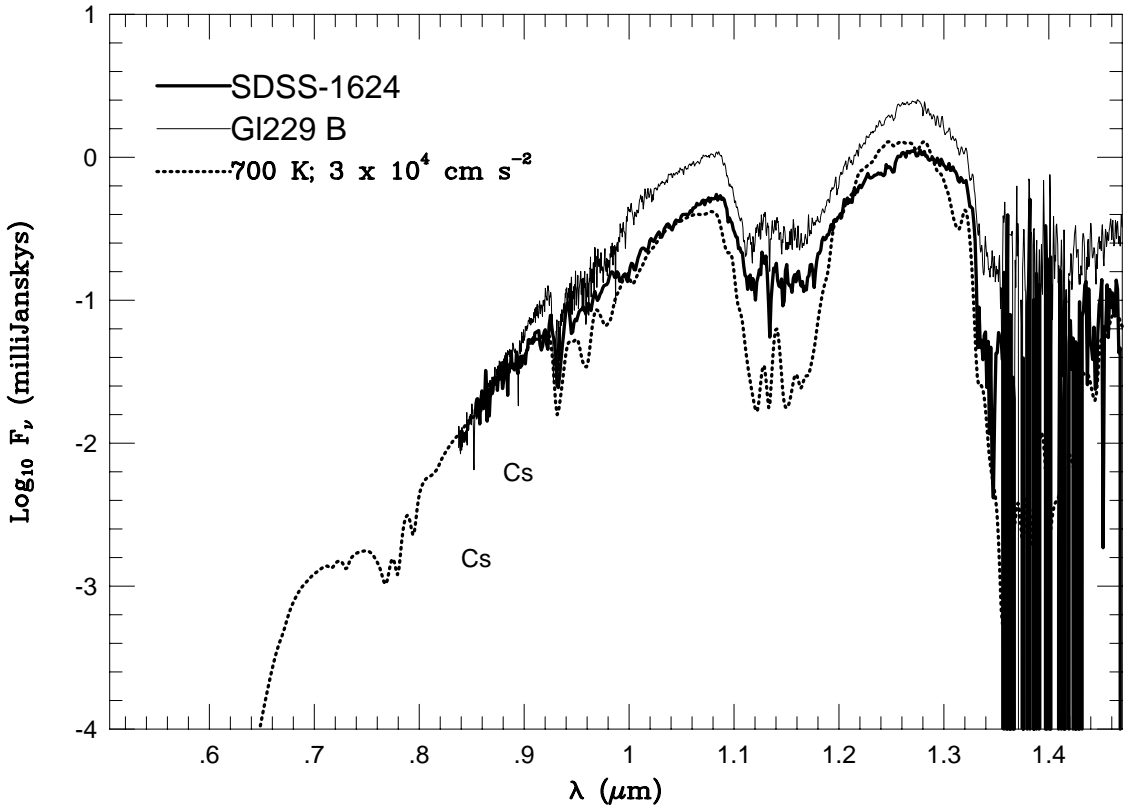


Fig. 8.— The log of the absolute flux ( $F_\nu$ ) in milliJanskys versus wavelength ( $\lambda$ ) in microns for the first Sloan T dwarf, SDSS 1624+00 (heavy solid line), from Strauss *et al.* (1999). The light solid line is Gliese 229B, while the dotted line is for a model with  $T_{\text{eff}} = 700$  K and  $g = 3 \times 10^4$  cm s $^{-2}$ . The core entropy of this theoretical model is lower than that for those that fit Gliese 229B. Both the model and the Sloan data have a shallower slope than Gliese 229B from 0.85  $\mu\text{m}$  to 1.0  $\mu\text{m}$  and weak cesium lines.